Crystallization and Stress Relaxation in Highly Stretched Samples of Natural Rubber and Its Synthetic Analogue

Masatoshi Tosaka,* Daisuke Kawakami, Kazunobu Senoo, and Shinzo Kohjiya

Institute for Chemical Research, Kyoto University, Uji, Kyoto 611-0011, Japan

Yuko Ikeda

Kyoto Institute of Technology, Matsugasaki, Kyoto 606-8585, Japan

Shigeyuki Toki and Benjamin S. Hsiao

Department of Chemistry, State University of New York at Stony Brook, New York 11794-3400

Received February 24, 2006; Revised Manuscript Received April 28, 2006

ABSTRACT: Vulcanizates of natural rubber (NR) and its synthetic analogue (IR) were quickly stretched to 6 times the original length. The post stretch relaxation of tensile stress and the development of strain-induced crystallization (SIC) were studied by simultaneous measurements of the stress and the diffraction intensities using the synchrotron X-ray source. In the range of 8 s, NR crystallized much faster than IR. Accordingly, the origin of the superior toughness of NR was thought to come from the ability of rapid SIC. Time constants of the post-stretch crystallization were estimated from the X-ray study. Then the crystallization time constants were used to decompose the contribution of SIC from the total magnitude of the post-stretch relaxation. The contribution of SIC was dominant for the total magnitude of the post-stretch relaxation during several seconds.

Introduction

Natural rubber (NR) is an indispensable material for many industrial and household applications,[1] especially for heavy-duty tires and quake-absorbing structures. This is mainly due to its outstanding tensile properties and the good crack growth resistance. NR is preferred also for medical products such as surgical gloves, because of its softness, extensibility, and the ability to form a very thin film having the complicated shape without any pinholes. Its synthetic analogue, namely synthetic *cis*-1,4-polyisoprene rubber (IR), cannot substitute for NR due to inferior toughness of the resulting products.

The superior physical properties of NR products would be related to the occurrence of strain-induced crystallization (SIC). For example, Trabelsi et al.[2] compared NR and IR having the same composition and reported the faster and higher crystallinity in NR. The induced crystallites may reinforce the material as filler particles. At the same time, the stress itself on the stretched rubber is reduced by the occurrence of SIC.[3−8] This is because the molecular chains in the crystallites adopt the extended conformation aligned in the stretching direction.[2,3,9−12] Thus, stress relaxation could be another mechanism that brings out the good physical properties of NR products. However, even in the case of cross-linked rubber, there are contributions not only from SIC but also from plastic flow (namely, the mutual slippage of molecular chains) in the experimentally measured values of stress relaxations. Because of the difficulty to estimate their relative contributions, the effect of the stress relaxation by SIC on the toughness of NR products has not been discussed so far.

We must also consider the rate of SIC, because the physical properties are not improved if SIC does not quickly occur in response to the mechanical load. The rate of SIC for the same rubber sample is accelerated by increasing strain ratio, α.[4,6,8] This is explained as below. With increasing α, the melting temperature increases.[10,13,14] The difference between ambient temperature and melting temperature, namely supercooling, correspondingly increases. Because the rate of polymer crystallization is largely affected by supercooling,[15] the acceleration of SIC by the increase in α is quite significant.

Network-chain density, ν, is another factor that may affect the rate of SIC. In the case of an unstretched sample (not SIC but thermally induced crystallization), the crystallization rates at low temperature were decelerated with the increase in ν.[16] For the stretched samples, Gent[6] and Trabelsi et al.[17] reported on the relationship between ν and the rate of SIC. Also in these studies, SIC was slower in samples with the higher ν. Note that these studies have observed SIC over a relatively long time under small α.

Although the response to the instantaneous mechanical load is important for a practical usage, former works on the kinetics of SIC have been performed mostly under the condition of small α and under long time scales ranging from several minutes to several months; we can hardly find the studies on this topic in the time scale of a few seconds or shorter. This is because the rate of SIC at high elongation is too fast for the measurements of wide-angle X-ray diffraction (WAXD). Probably, the only exception was the work by Mitchell and Meier.[18] They succeeded in measuring the excess temperature rise due to SIC and estimated its time constant to be around 50 ms. However, their experimental method was not applicable for the phenomenon longer than one second or more, because the excess heat is dissipated in a few seconds, leading to inaccurate analysis of SIC for the longer time.

In this paper, we report the post-stretching SIC behavior in vulcanized NR and IR samples after fast deformation. High-cycle WAXD experiments were conducted using a synchrotron light source along with simultaneous tensile measurements; the cycle of WAXD acquisition was shorter than 0.1 s. The

* Corresponding author. E-mail: tosaka@scl.kyoto-u.ac.jp. Telephone: +81-774-38-3062. Fax: +81-774-38-3069.

10.1021/ma060407+ CCC: $33.50
Published on Web 06/21/2006

Table 1. Recipes and Cure Conditions of Vulcanized Rubber Samples

sample code	rubber[a] (part)	stearic acid (part)	active ZnO (part)	CBS[b] (part)	sulfur (part)	total (part)	curing time (min)	network chain density $\times 10^4$ (mol/cm^3)
NR1	100	2	1	3	4.5	110.5	10	2.12
NR2	100	2	1	2	3	108	12	1.78
NR3	100	2	1	1.5	2.25	106.75	12	1.46
NR4	100	2	1	1	1.5	105.5	17	1.31
NR5	100	2	1	0.75	1.125	104.88	17	1.01
NR9	100	2	1	0.67	1	104.67	23	0.54
NR10	100	2	1	0.5	0.75	104.25	23	0.37
IR1	100	2	1	3	4.5	110.5	17	1.99
IR2	100	2	1	2	3	108	17	1.66
IR3	100	2	1	1.5	2.25	106.75	24	1.36
IR4	100	2	1	1	1.5	105.5	24	1.29
IR5	100	2	1	0.75	1.125	104.88	30	1.03

[a] NR is RSS No. 1 from Malaysia and IR is IR2200 from JSR. [b] *N*-cyclohexyl-2-benzothiazole sulfenamide, curing temperature with sulfur 140 °C.

Table 2. Exposure Conditions for the WAXD Study

condition	exposure length (s)	cycle length (s)	max. value of t (s)	applied samples
1	0.036	0.083	8	all
2	0.036	1	30	all
3	0.100	30	1800	NR1, NR4, NR5, NR10, IR2, IR4, IR5

relationship between ν and rate of SIC, especially in the range of several seconds, was experimentally examined. Then the contribution of SIC in the total magnitude of stress relaxation was quantitatively discussed.

Experimental Section

Vulcanized NR (RSS No. 1) and IR (IR2200, JSR) samples were prepared according to the recipes and cure conditions shown in Table 1. The ν values are also included in this table. The preparation and characterization procedures of the vulcanized rubber sheets (1 mm thickness) have been reported in our previous works.[10,19] The ν values of NR1−NR5 and IR1−IR5 are in the range of general purpose rubber, while NR 9 and NR10 have unusually low ν values as rubber products, and accordingly, they are rather soft and sticky. Ring-shaped specimens[20] were die-cut from the sheets and used for the experiments. The inner and outer diameters of the specimens were 11.7 and 13.7 mm, respectively (ca. 40 mm circumference).

The experiments were performed at BL-40XU beamline in SPring-8, Japan. A custom-made tensile tester was situated on the beamline where ambient temperature was controlled at 25 °C. This tensile tester could stretch the specimen symmetrically to examine almost the same position of the specimen by X-ray diffraction/scattering.[20] The specimen was stretched to a predetermined strain ratio, α_s, and immediately stopped. The maximum speed of the tensile tester (500 mm/min) was used. As initial length of the ring-shaped specimen corresponds to the half of its circumference, the strain rate was 25 min^{-1} when the entire specimen deformed uniformly. Tensile stress, $\sigma(t)$, and WAXD patterns were recorded simultaneously during and after the stretching as functions of elapsed time, t (s). In this paper, we consistently describe t in units of seconds and define the origin of the elapsed time ($t = 0$) as the moment when the stretching was stopped. Intensity of the incident X-ray was attenuated using a rotating slit equipped by the beamline in order to avoid radiation damage of the specimen. Accordingly, the incident beam was not continuous but pulsed. Acquisition of the two-dimensional WAXD patterns was repeated every 83 ms (36 ms exposure + 47 ms data transfer) using a Hamamatsu C4880−80 CCD camera until $t = 8$. The acquisition started 1 s before stopping ($t = -1$) to reduce total number of the data file. Additionally, experiments for longer time were performed under the conditions listed in Table 2. The specimens were exchanged for each measurement. The wavelength was 0.0832 nm and the camera length was ca. 180 mm.

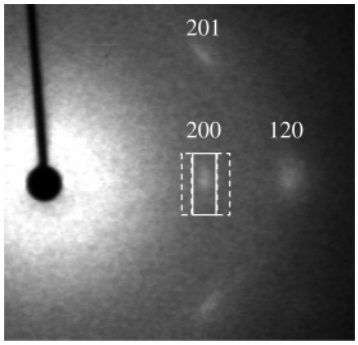

Figure 1. Major reflections from the oriented crystals in stretched NR4. The rectangular regions used for the estimation of $I(t)$ are indicated. The area of the rectangle designated by solid lines is equal to the total area of the two rectangles designated by broken lines.

Processing of the WAXD Data

As the quality of the images were not enough to allow us to discuss, e.g., the crystallite size,[10] only the development of the relative intensity of the 200 reflection was evaluated. In this experiment, the apparent intensity of incident X-ray was different for every WAXD pattern, because the total dose to record the WAXD pattern changed due to the modulation between the image-acquisition cycle and the rotation cycle of the attenuating slit. Therefore, the intensity of the 200 reflection had to be normalized using an internal standard. Consequently, integrated intensity of two rectangular regions including the 200 reflections (indicated by solid lines in Figure 1) was normalized using integrated intensity of rectangular regions on the both sides (indicated by broken lines in Figure 1). Thus, estimated value, $I(t)$, is about 1 (or a little smaller due to the distribution of the halo) when the specimen is amorphous, and increases with crystallinity. We assumed the linear relationship between $I(t)$ and crystallinity for the subsequent discussion.

Results and Discussion

We performed some pilot studies beforehand using dumbbell-shaped specimens and different experimental setup to explore the relationship between the predetermined strain ratio to hold the specimen, α_s, and the degree of post-stretch crystallization. This experiment itself was not successful because of inhomogeneous extension of the dumbbell-shaped specimen. However, we could find the clearest evidences of development of crystallinity under the condition of $\alpha_s = 6$. Accordingly, we determined to study the case of this α_s. (All of the data in this paper were obtained by the experiments using the ring-shaped specimens described in the Experimental Section.)

Figure 2 shows an example of overall change of $\sigma(t)$ and the WAXD patterns. During stretching ($t < 0$), the tensile stress

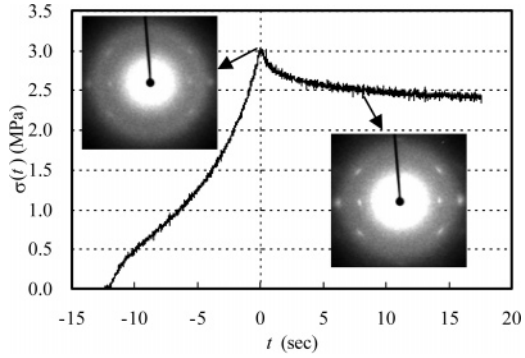

Figure 2. Overall change of tensile stress and corresponding WAXD patterns in the case of NR4.

increased with time. When the stretching was stopped at $\alpha = \alpha_s$ (=6), the stress decreased immediately, and the slower stress relaxation continued. As shown in the inset of Figure 2, NR4 (and some other samples) already crystallized at $t = 0$. This means that there are quite rapid components of SIC in some of the samples,[18] to which the current study cannot catch up due to instrumental limitation. Then the intensity of crystalline reflections in the WAXD pattern increased after stopping ($t > 0$). This paper handles mainly the latter component of SIC which develops in several seconds.

Crystallization Behaviors of NR and IR. Development of crystallinity was quantitatively evaluated using $I(t)$ values. Figure 3a shows the crystallization behaviors of NR samples during and after stretching ($t \leq 8$). Samples with relatively high ν (NR1−NR4) significantly crystallized during stretching ($t < 0$). After stopping, $I(t)$ of all samples gradually increased. Figure 4a shows the results for longer time (until 30 min; $t \leq 1800$). The crystallinity increased almost linearly with logarithm of elapsed time. An interesting finding is that the rate of SIC is faster for the samples having the higher ν. This trend is opposite to cold crystallization of unstretched samples[16] and to SIC under small α_s (≤ 4).[6,17] We have proposed that a certain fraction of the stretched network chains would play the role of nuclei for SIC.[10] As there should be more nuclei in stretched rubber with the higher ν values, SIC is accelerated and the trend in Figure 4a would appear under our experimental condition. On the other hand, samples with higher ν contain more cross-linking which cannot be included in crystallites. Under the conditions of small or null α_s, the necessity to exclude the cross-linking from crystallizing molecular chains would retard crystallization, and at the same time, would diminish the attainable crystallinity.[2,6,16] In Figure 4a, the crystallization of NR1 that has the highest ν is decelerated earlier than other samples, probably due to the lower attainable crystallinity.

In the case of IR, SIC proceeds at much slower rate. Figures 3b and 4b show the crystallization behaviors of IR samples. As shown in Figure 3b, even the sample with the highest ν (IR1) hardly crystallized during stretching. Compared to NR, IR required longer induction time (Figure 4b).[21] Gent et al.[8] reported that tear strength under slow deformation is not so different between NR and IR, but under fast deformation, IR showed markedly lower tear strength. According to the current results, the superior tear strength of NR under fast deformation rate would originate from the ability of rapid SIC. Under relatively fast deformation, IR could fracture before the occurrence of SIC, while NR will have chance to reinforce itself by quick formation of the strain-induced crystallites.

Note that vulcanized NR has higher melting temperature than IR at every strain ratio.[2,8] Accordingly, at sufficiently large α,

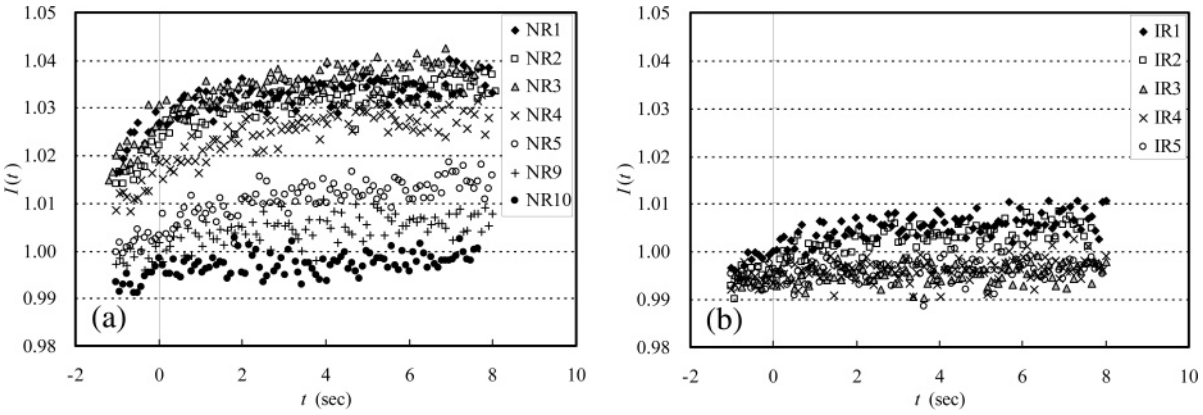

Figure 3. Crystallization behaviors in 8 s for (a) NR and (b) IR samples.

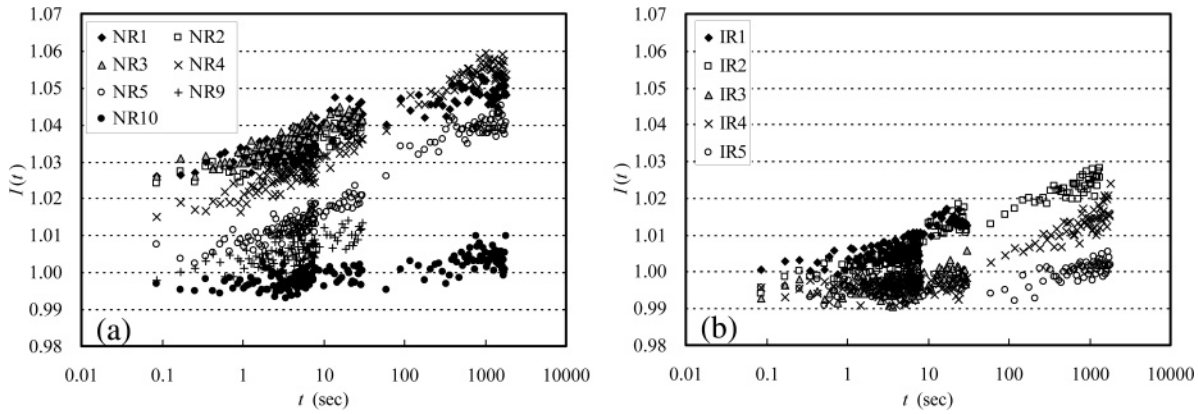

Figure 4. Crystallization behaviors until 30 min of elapsed time ($t \leq 1800$) for (a) NR and (b) IR samples. The horizontal axis is in the logarithmic scale of elapsed time (sec). The data from conditions 1−3 in Table 2 were combined.

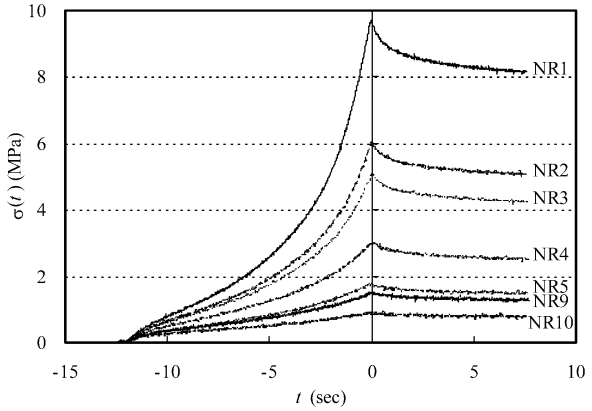

Figure 5. Tensile stress change for NR ($t \leq 8$) before the normalization.

supercooling for NR is larger than that of IR under the same condition. This should be the reason for the faster SIC of NR.

In some of our previous works on cyclic deformation of cross-linked NR, we paid attention to values of α at which crystallization starts.[10,19,20,22,23] The discussions presented there implicitly assumed that the rate of SIC is high enough so that we can ignore the dynamic effect on the occurrence of SIC. As shown in Figures 3a and 4a, SIC of NR was quite fast that we could not detect the induction time. Thus, we were convinced of our assumption in the previous works.

Stress Relaxation. The raw data of tensile stress, $\sigma(t)$, for NR samples are plotted in Figure 5. As shown in Figure 2, we can observe the stress relaxation for all the samples in the post-stretching stage. This is partly because SIC stabilizes the stretched molecular chains in the tensile direction.[3,9,10] However, like noncrystalline rubber materials, stress relaxation will occur due to another reason. That is to say, the stress relaxation reflects both the effects of SIC and plastic flow. The relative contribution of these two factors was expected to vary with ν. Accordingly, we compared the degree of stress relaxation for the samples with different ν. As the absolute values of tensile stress were quite different among the samples with different ν, the degree of stress relaxation was compared after normalization using the maximum stress value at $t = 0$, namely $\sigma(0)$.

Figure 6 shows the normalized stress values, $\sigma(t)/\sigma(0)$. In the case of NR, the normalized stress changed almost linearly after $t =$ ca. 0.1 in the logarithmic scale of time. On the other hand, somewhat gradual change of the slope was recognized for IR (Figure 6b). It is interesting to find that, after normalization by $\sigma(0)$, the plots for each sample almost overlap regardless to the difference in ν, while there is a definite difference between NR and IR.

Decomposition of Stress Relaxation. To consider the contributions of SIC and plastic flow separately and quantitatively, we formulated the stress change as

$$\sigma(t) = \sigma(0) - \sigma_{i1}[1 - \exp(-t/\tau_1)] - \sigma_{i2}[1 - \exp(-t/\tau_2)] \quad (1)$$

In the right side of eq 1, the first term is the maximum tensile stress at $t = 0$, and the second and the third terms corresponds to the stress relaxations due to crystallization and plastic flow, respectively; σ_{i1} and σ_{i2} are magnitudes of relaxation, and τ_1 and τ_2 are time constants, of these components. The function form in the second and third terms, namely $[1 - \exp(-t/\tau)]$, is usually used to describe viscoelastic deformation.[24]

We attempted to decompose the post-stretch stress data into contributions from crystallization and plastic flow by fitting the experimental data with eq 1. The parameters to be determined were σ_{i1}, σ_{i2}, τ_1 and τ_2, while $\sigma(0)$ was a known value. However, our first trial of the fitting was not successful and the final values were scattered from sample to sample, probably because the number of unknown parameters (namely, the degree of freedom) was too large. It was necessary to reduce the degree of freedom. Here, the crystallization time constant τ_1 should be solely estimated from the WAXD study. By using this value, the degree of freedom for fitting the stress data by eq 1 is reduced, and accordingly, the reliability of the final result would increase. Thus, the $I(t)$ data in Figure 3a ($0 \leq t \leq 8$) were fit beforehand using the function

$$I(t) = I(0) + I_i[1 - \exp(-t/\tau_1)] \quad (2)$$

to estimate τ_1; $I(0)$ is the $I(t)$ value at $t = 0$, and I_i is the magnitude of the intensity increment during the post-stretch stage. Then the stress data in Figure 5 ($0 \leq t \leq 8$) were fit by eq 1 using the predetermined τ_1 and $\sigma(0)$ values to estimate σ_{i1}, σ_{i2}, and τ_2. Finally, σ_{i1} was normalized by $\sigma(0)$ to compare the samples with different ν. If the decomposition using eq 1 is successful, I_i (the magnitude of the diffraction intensity change due to crystallization) and $\sigma_{i1}/\sigma(0)$ (the magnitude of the stress relaxation due to crystallization) should have linear relationship.

Figure 7 plots I_i and $\sigma_{i1}/\sigma(0)$ against ν for NR. (The data in the range $0 \leq t \leq 8$ were used for the fitting.) Almost the same trend (which will be discussed shortly) is found for I_i and $\sigma_{i1}/\sigma(0)$. The relationship between I_i and $\sigma_{i1}/\sigma(0)$ is shown in Figure 8. The correlation coefficient between the two quantities was

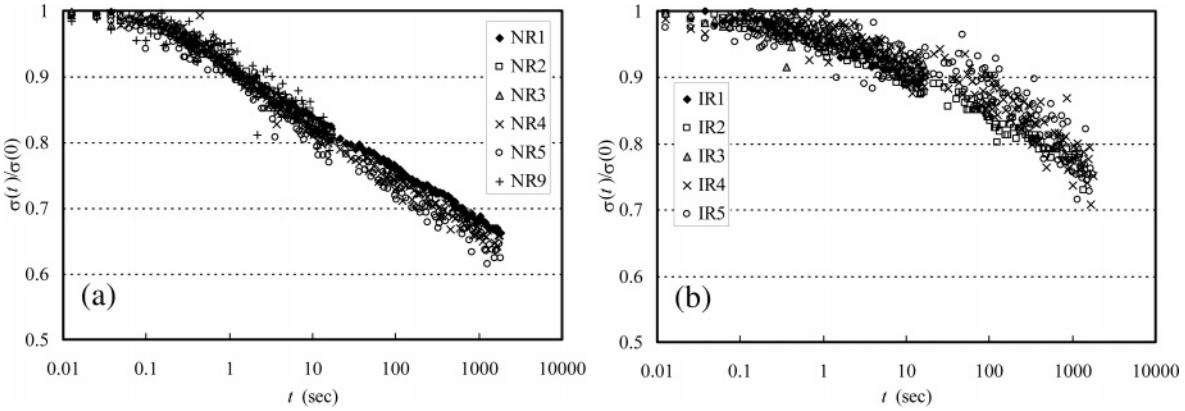

Figure 6. Tensile stress normalized by $\sigma(0)$ for (a) NR and (b) IR. The data from conditions 1−3 in Table 2 were combined. To improve the visibility, some of the data are skipped in the plots. (For the analysis in the main text, the complete set of data was used.) Because of a poor *S*/*N* ratio, the data for NR10 are not included.

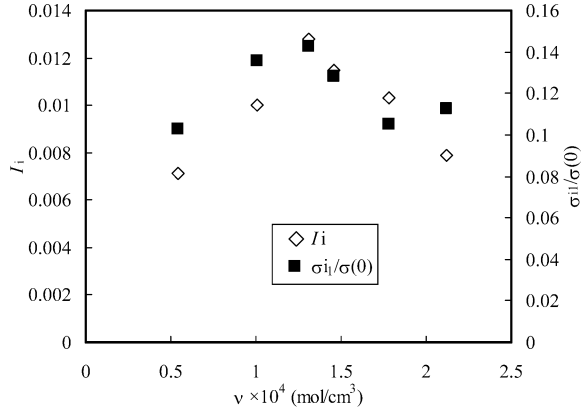

Figure 7. Dependence of I_i and $\sigma_{i1}/\sigma(0)$ on ν for NR. The data in the range $0 \le t \le 8$ were used.

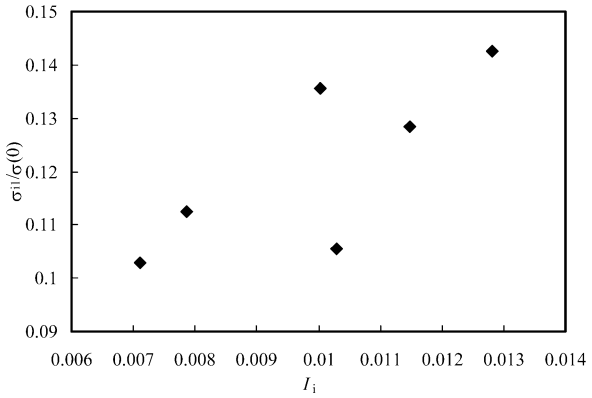

Figure 8. Relationship between I_i and $\sigma_{i1}/\sigma(0)$ for NR. The data in the range $0 \le t \le 8$ were used.

Table 3. Final Parameters Obtained by the Fitting of $I(t)$ and $\sigma(t)$ Curves

sample code	$\sigma(0)$	σ_{i1}	τ_1	σ_{i2}	τ_2
NR1	9.43	1.061	2.35	0.224	0.506
NR2	5.87	0.619	3.05	0.228	0.663
NR3	4.96	0.637	2.31	0.088	0.469
NR4	2.96	0.422	2.16	0.025	0.452
NR5	1.72	0.233	2.87	0.028	0.426
NR9	1.47	0.151	5.57	0.074	1.181

0.84, which value passes the correlation test of 5% of significant level. That is to say, we can regard I_i and $\sigma_{i1}/\sigma(0)$ to change linearly with each other. Therefore, we judged the stress relaxation data to be successfully decomposed into contributions of SIC and plastic flow. The final values of the fitting parameters are listed in Table 3. We notice that the values of τ_2 were smaller than τ_1, i.e., the decomposed components of the plastic flow in the current analysis had the smaller time constants than SIC.

Figure 9 shows the relative contribution of SIC to the total magnitude of stress relaxation (namely, $\sigma_{i1}/(\sigma_{i1} + \sigma_{i2})$) in the range $0 \le t \le 8$. Under this experimental condition (strain rate $= 25$ min^{-1}, $\alpha_s = 6$, ambient temperature $= 25$ °C), SIC contributed to ca. 65−95% of the total magnitude of post-stretch stress relaxation for NR. In each of Figures 7 and 9, there is a maximum around $\nu = 1.3$. The decrease on the smaller ν side is, as is noticed from Figures 3a and 4a, due to the slower rate of SIC. On the other hand, the behavior on the larger ν side is explained by two reasons. One is the lower attainable crystallinity due to the higher ν. The other reason is that the SIC has progressed during stretching, and as a result, less amount of crystallizable chains were left for the post-stretching stage. That is to say, the real contribution of SIC to the stress relaxation should be much larger.

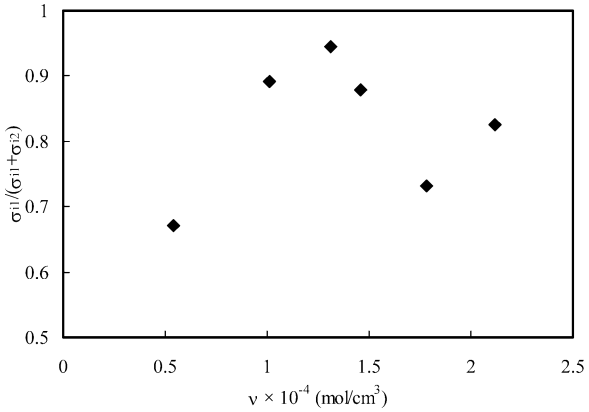

Figure 9. Relative contribution of SIC to the total magnitude of stress relaxation. The data in the range $0 \le t \le 8$ were used.

In this way, we could quantitatively analyze SIC and corresponding stress relaxation for NR. In the case of IR2−IR5 and NR10, the changes in the absolute values of $I(t)$ and $\sigma(t)$ were so small that they were buried in the noise. Accordingly, the curve fitting using eqs 1 and 2 was not successful for these samples. However, the smaller magnitude of post-stretch stress relaxation in IR further supports the reliability of our analysis for NR. On the basis of our analysis, if SIC did not occur, the magnitude of stress relaxation will be reduced. This situation corresponds to the case of IR. As shown in Figure 3b, SIC of IR hardly proceeded in the short range of time. Therefore, the magnitude of stress relaxation in the range $t \le 8$ would have been smaller for IR (Figure 6b). The definite difference between parts a and b of Figure 6 would have come from the different rates of SIC between NR and IR.

Conclusion

The high-cycle synchrotron WAXD study revealed that the NR samples, of which ν values are in the range of general purpose rubber, rapidly respond to fast deformation by forming strain-induced crystallites. On the other hand, the response of the IR samples was comparatively slow. Interestingly, the rate of SIC was the faster for the samples with the higher ν, which is the opposite trend found in the former works.[6,16] This means that the current study has provided significant information for the unique SIC behavior in short period of time. The ability, found exclusively in NR, of the rapid SIC and its reinforcing effect would be the important factor for the inimitable toughness of NR.

By the combination analysis of the WAXD pattern and the tensile strength, contributions of SIC and plastic flow to the total magnitude of stress relaxation could be successfully decomposed. In the short range of time, the contribution of SIC was found to be dominant. That is to say, for a tensile strain, SIC plays an important role to reduce the stress. This should be another factor that leads to the toughness of NR.

Although the current analysis was successful in the case of $\alpha_s = 6$, the maximum stretching rate of the tensile tester limited the accessible range of α_s to estimate the contribution of SIC. For example, a similar experiment under the condition of $\alpha_s = 7$ has been conducted. In this case, however, SIC progressed considerably during stretching; the relative weight of post-stretch SIC was too small for the meaningful discussion. A novel tensile tester that can stretch the specimen at much faster rate will be helpful to overcome this problem.

Acknowledgment. This work was supported partly by a Grant-in-Aid for Scientific Research (B)(2), No. 15404011, from

CDV

Japan Society for the Promotion of Science, partly by the Research Grants from President of KIT (to Y.I.), and partly by National Science Foundation (DMR-0405432) to the Stony Brook team. The synchrotron WAXD experiments were performed at the SPring-8 with the approval of the Japan Synchrotron Radiation Research Institute (JASRI) (Proposal No. 2003B0664-ND1b-np, 2004A0388-ND1b-np, 2005A0425-ND1b-np).

References and Notes

(1) Allen, P. W.; Jones, K. P. In *Natural Rubber Science and Technology*; Roberts, A. D., Eds.; Oxford University Press: Oxford, U.K., 1988; pp 1−34.
(2) Trabelsi, S.; Albouy, P.-A.; Rault, J. *Rubber Chem. Technol.* **2004**, *77*, 303−316.
(3) Miyamoto, Y.; Yamao, H.; Sekimoto, K. *Macromolecules* **2003**, *36*, 6462−6471.
(4) Kim, H.-G.; Mandelkern, L. *J. Polym. Sci., Part A-2* **1968**, *6*, 181−196.
(5) Gent, A. N.; Zhang, L.-Q. *J. Polym. Sci., Part B: Polym. Phys.* **2001**, *39*, 811−817.
(6) Gent, A. N. *Trans Faraday Soc.* **1954**, *50*, 521−533.
(7) Toki, S.; Sics, I.; Hsiao, B. S.; Tosaka, M.; Poompradub, S.; Ikeda, Y.; Kohjiya, S. *Macromolecules* **2005**, *38*, 7064−7073.
(8) Gent, A. N.; Kawahara, S.; Zhao, J. *Rubber Chem. Technol.* **1998**, *71*, 668−678.
(9) Flory, P. J. *J. Chem. Phys.* **1947**, *15*, 397−408.
(10) Tosaka, M.; Murakami, S.; Poompradub, S.; Kohjiya, S.; Ikeda, Y.; Toki, S.; Sics, I.; Hsiao, B. S. *Macromolecules* **2004**, *37*, 3299−3309.
(11) Toki, S.; Sics, I.; Ran, S.; Liu, L.; Hsiao, B. S.; Murakami, S.; Tosaka, M.; Kohjiya, S.; Poompradub, S.; Ikeda, Y.; Tsou, A. H. *Rubber Chem. Technol.* **2004**, *77*, 317−335.
(12) Toki, S.; Fujimaki, T.; Okuyama, M. *Polymer* **2000**, *41*, 5423−5429.
(13) Yamamoto, M.; White, J. L. *J. Polym. Sci., Part A-2* **1971**, *9*, 1399−1415.
(14) Tutorsky, I. A.; Shumanov, L. A.; Dogadkin, B. A. *Polymer* **1968**, *9*, 413−418.
(15) Hoffman, J. D.; Miller, R. L. *Polymer* **1997**, *38*, 3151−3212.
(16) Bekkedahl, N.; Wood, L. A. *Ind. Eng. Chem.* **1941**, *33*, 381−384.
(17) Trabelsi, S.; Albouy, P.-A.; Rault, J. *Macromolecules* **2003**, *36*, 7624−7639.
(18) Mitchell, J. C.; Meier, D. J. *J. Polym. Sci., A-2* **1968**, *6*, 1689−1703.
(19) Tosaka, M.; Kohjiya, S.; Murakami, S.; Poompradub, S.; Ikeda, Y.; Toki, S.; Sics, I.; Hsiao, B. S. *Rubber Chem. Technol.* **2004**, *77*, 711−723.
(20) Ikeda, Y.; Yasuda, Y.; Makino, S.; Yamamoto, S.; Tosaka, M.; Senoo, K.; Kohjiya, S. Submitted to *Polymer*.
(21) Toki, S.; Sics, I.; Ran, S.; Liu, L.; Hsiao, B. S. *Polymer* **2003**, *44*, 6003−6011.
(22) Poompradub, S.; Tosaka, M.; Kohjiya, S.; Ikeda, Y.; Toki, S.; Sics, I.; Hsiao, B. S. *J. Appl. Phys.* **2005**, *97*, 103529/1−103529/9.
(23) Ikeda, Y. *Kautsch. Gummi Kunstst.* **2005**, *58*, 455−460.
(24) Billmeyer, J.; Fred., W. *Textbook of Polymer Science*, 3rd ed.; Wiley-Interscience: New York, 1984.

MA060407+